Mon. Not. R. Astron. Soc. **000**, 1-13 (2001) Printed 1 February 2008 (MN LATEX style file v1.4)

# X-Rays from Isolated Black Holes in the Milky Way

Eric Agol⋆ and Marc Kamionkowski
*California Institute of Technology, Mail Code 130-33, Pasadena, CA 91125 USA*

August 2001



**ABSTRACT**
Galactic stellar-population-synthesis models, chemical-enrichment models, and long-duration Bulge microlensing events indicate about $N_{\rm tot} = 10^8 - 10^9$ stellar-mass black holes reside in our Galaxy. We study X-ray emission from accretion from the interstellar medium on to isolated black holes. Although isolated black holes may be fewer in number than neutron stars, $N_{NS} \sim 10^9$, their higher masses, $\langle M \rangle \sim 9{\rm M}_\odot$, and smaller space velocities, $\sigma_v \sim 40$ km s$^{-1}$ result in Bondi-Hoyle accretion rates $\sim 4 \times 10^3$ times higher than for neutron stars. We estimate that $\sim 10^4$ isolated black holes within the Milky Way should accrete at $\dot{M} > 10^{15}$ g s$^{-1}$, comparable to accretion rates inferred for black-hole X-ray binaries given a total number of black holes $N_{\rm tot} = N_9 10^9$. If black holes accrete at efficiencies only $\sim 10^{-4}(N_{NS}/N_{\rm tot})^{0.8}$ of the neutron-star accretion efficiency, a comparable number of each may be detectable. We make predictions for the number of isolated accreting black holes in our Galaxy which can be detected with X-ray surveys as a function of efficiency, concluding that all-sky surveys at a depth of $F = F_{-15}10^{-15}$ erg cm$^{-2}$ s$^{-1}$ dex$^{-1}$ can find $N(>F) \sim 10^4 N_9 (F_{-15}/\epsilon_{-5})^{-1.2}$ isolated accreting black holes for a velocity dispersion of 40 km s$^{-1}$ and X-ray accretion efficiency of $\epsilon = \epsilon_{-5}10^{-5}$. Deeper surveys of the Galactic plane with *Chandra* or *XMM-Newton* may find tens of these objects per year, depending on the efficiency. We argue that a minimum mass can be derived for microlensing black-hole candidates if they are detected in the X-ray.

**Key words:** accretion, accretion discs — black hole physics — Galaxy: stellar content — X-rays: ISM, stars

## 1 INTRODUCTION

A black hole may only be detected via its interactions with surrounding matter or light. Black holes in binary-star systems are strong and transient X-ray sources fed by accretion from a stellar companion. However, isolated black holes—that is, black holes without companions or black holes in wide binaries—can easily escape detection. These may constitute the majority of the population of black holes since the fraction in close binaries with $a < 100$ AU is $\sim 0.01$ based stellar evolution calculations for massive star binaries (Chris Fryer, priv. comm. 2001). Young isolated neutron stars are much easier to detect as pulsars, but once the magnetic field, spin, and thermal energy decay away, an old neutron star becomes as invisible as a black hole. Several authors (Ostriker, Rees & Silk 1970, Treves & Colpi 1991, Blaes & Madau 1993) have proposed searching for isolated old neutron stars lit up by accreting matter from the interstellar medium (ISM). A tenth of the rest-mass energy of the accreting gas can be directly converted to luminosity assuming that all the accreted material is thermalised as it hits the neutron-star surface. These predictions motivated searches that turned up several isolated neutron-star candidates (Stocke et al. 1995, Walter et al. 1996, Wang 1997, Schwope et al. 1999); however, it is possible that these are young cooling neutron stars powered by processes other than accretion (Treves et al. 2000).

The known Galactic black-hole X-ray-binary population has a velocity dispersion smaller by a factor of $\sim 5$ than neutron stars (Hansen & Phinney 1997, White & van Paradijs 1996, van Paradijs & White 1995) and average mass larger by a factor of $\sim 6$ (see below and Bailyn et al. 1998, Thorsett & Chakrabarty 1999). The accretion rate for an object of mass $M$ accreting from the interstellar medium is determined by the Bondi-Hoyle formula (Bondi & Hoyle 1944),

$$\dot{M} = \frac{\lambda 4\pi G^2 M^2 n \mu}{(v^2 + c_s^2)^{3/2}}, \quad (1)$$

⋆ Chandra Fellow, Email: agol@tapir.caltech.edu

where $v$ is the velocity of the black hole with respect to the local interstellar medium, $n$ is the number density of hydrogen in the interstellar medium, $\mu = \rho/n$ where $\rho$ is the particle mass density, $c_s$ is the sound speed of the interstellar medium, and $\lambda$ is a parameter of order unity (we set $\lambda = 1$ hereafter). Assuming that isolated black holes have the same mass range and velocity dispersion as black holes in X-ray binaries, one would expect the typical accretion rate on to isolated black holes from the ISM to be larger by a factor of $\sim 4 \times 10^3$ compared to neutron stars. The expected detection rate of isolated black holes accreting from the ISM may be reduced as the number of black holes in our Galaxy may be smaller by a factor of $\sim 10$ than the number of neutron stars, and the lack of a hard surface may result in lower luminosities for black holes accreting at small accretion rates. Garcia et al. (2001) argue that black holes have quiescent X-ray efficiencies $\sim 10^{-2}$ of neutron stars; however, Bildsten & Rutledge (2000) argue that the detected X-rays may have nothing to do with accretion, and V404 Cyg is an exception to this rule indicating that there may be a wide range of accretion efficiencies. If black holes do have a reduced efficiency compared to neutron stars, this reduction can be compensated by the larger accretion rates and the smaller scale height of black holes which increases their number density in the mid-plane where most of the interstellar gas mass is located. Black holes do not have an intrinsic magnetic field, so accretion can proceed uninhibited by magnetic pressure or torque. Thus, we are motivated to compute the expected numbers and accretion rates of isolated black holes in our Galaxy.

The problem of black holes accreting from the interstellar medium has been considered by several authors. We approach the problem in a different way from previous authors (listed below) by using the properties of black-hole X-ray binaries and black-hole microlensing candidates to constrain the phase-space distribution of black holes within the entire Galactic disc (discussed in detail in Agol & Kamionkowski 2001, in preparation), while considering the properties of all phases of the ISM, deriving the distribution of accretion rates including radiative pre-heating, and finally deriving the distribution of X-ray fluxes. Grindlay (1978) considered spherical-accretion models for X-ray sources now known to be accreting from companions. Carr (1979) estimated the luminosity of black holes in the galactic disc, but did not predict their detection probability. McDowell (1985) computed the visual and infrared fluxes of black holes accreting spherically from molecular clouds, but only out to 150 pc. Campana & Pardi (1993) computed the fluxes of black holes within the disc of the Galaxy accreting spherically from molecular clouds, without computing the probability distribution of accretion rates. Heckler & Kolb (1996) computed the fluxes of a putative halo population of black holes accreting spherically while passing within 10 pc of the Sun. The large velocities, low densities, and large scale heights of a halo population greatly reduces the number of black holes at a given accretion rate. Popov & Prokhorov (1998) took into account the spatial distribution of the warm interstellar medium, assuming the black holes receive a kick velocity at birth of $\sim 200$ km s$^{-1}$, which greatly reduces the accretion rates. Fujita et al. (1998) computed the fluxes of black holes in the disc accreting via an advection-dominated accretion flow at a distance of 400 pc (the Orion cloud) for a few velocities, without computing the full probability distribution. Grindlay et al. (2001) estimate that of order $10^3$ black holes in molecular clouds might be detectable by the proposed Energetic X-ray Imaging Survey Telescope (*EXIST*) experiment based on an accretion efficiency of $10^{-2}$.

The spectrum of an accreting black hole has been computed in the spherical-accretion limit (Ipser & Price 1977, 1982, 1983); however, as we show below, the accreted material will possess non-zero angular momentum, possibly forming an accretion disc which may increase the efficiency of accretion. Thus, we parameterize our results in terms of the unknown accretion efficiency.

In section 2 we summarize the known properties of binary and isolated black holes and their distribution in phase space. In section 3 we estimate the accreted angular momentum, discuss the range of accretion efficiencies, and discuss the effects of radiative feedback. In section 4 we discuss the properties of the interstellar medium necessary for computing the accretion rates of black holes. In section 5 we compute the distribution of accretion rates and luminosities for black holes within the disc of the galaxy. In section 6 we estimate the detection rates of black holes under the persistent and transient assumptions, and then we predict the fluxes as a function of distance for the three candidate black-hole microlenses. Finally in section 7 we summarize.

## 2 ISOLATED BLACK HOLES IN OUR GALAXY

The relevant results from Agol & Kamionkowski (2001) on the number and distribution of black holes within the Galaxy are summarized here.

### 2.1 Number of black holes

Three microlensing events toward the Galactic Bulge have been found by the MACHO and OGLE teams (Bennett et al. 2001, Mao et al. 2001). These events are of long enough duration ($> 1$ year) to observe variations in the microlensing light curve due to the motion of the Earth around the Sun, an effect known as microlensing parallax. This breaks some of the degeneracy between distance, velocity, and mass of the lensing object; when combined with a model for the velocity and number density of black holes in the Galaxy, this results in an estimate of the likely mass of the lensing objects. In all three cases, the objects likely have masses greater than $3M_\odot$, while they are not detected as main-sequence stars, leading to the conclusion that they are most likely black holes (Bennett et al. 2001, Agol & Kamionkowski 2001). Based on the probability of microlensing toward the Bulge and assuming that isolated black holes have the same scale height as black holes in binaries, one concludes that the total number of black holes in the Milky Way disk is $2 \times 10^8 < N_{\rm tot}(f/0.2) < 4 \times 10^9$ at 95 per cent confidence, for a

microlensing detection efficiency $f$, estimated to be 20 per cent (Alcock et al. 2000). Given the uncertainty in these estimates, we will make predictions based on $N_{\rm tot} = N_9 10^9$ black holes, and note that our results scale with $N_9$.

As discussed below, there is some evidence that the velocity dispersion of isolated black holes is similar to that of the stellar disk. We thus assume that the number density of black holes is distributed as

$$N_{\rm BH} = N_\odot \exp\left[-\frac{|Z|}{H} - \frac{(R-R_\odot)}{R_{\rm disc}}\right], \tag{2}$$

where $N_\odot$ is the number density at the solar circle, $Z$ and $R$ are the cylindrical Galactic coordinates, $R_\odot = 8$ kpc is the distance to Galactic centre, $H$ and $R_{\rm disc}$ are the disc scale height and scale length. We will assume that the black-hole disc scale height is $H = 375$ pc and scale length is $R_{\rm disc} = 3$ kpc. This implies a local number density of $N_\odot = 1.64\times10^5 N_9 (H/375{\rm pc})^{-1}$.

### 2.2 Velocity distribution of isolated black holes

White & van Paradijs (1996) have estimated that the rms distance from the Galactic plane for black-hole X-ray binaries, $z_{\rm rms}$, is about 450 pc, which corresponds to a scale height of $H \sim 320$ pc and velocity dispersion of $\sigma_v \sim 40$ km s$^{-1}$. This is consistent with the radial-velocity measurements of low-mass black-hole X-ray binaries when corrected for Galactic rotation (Brandt et al. 1995, Nelemans et al. 1999), with the exception of GRS 1655-40 which has $v_r = -114$ km s$^{-1}$. We have improved on the work by White & van Paradijs (1996) by using a maximum-likelihood analysis based on 19 black-hole X-ray binaries, concluding that $H = 375^{+135}_{-60}$ pc (Agol & Kamionkowski 2001). In addition, the three isolated black holes have a vertical velocity dispersion of $\sigma_z < 27$ km s$^{-1}$ at 95 per cent confidence, indicating that their kinematics, and thus spatial distribution, is similar to that of black holes in X-ray binaries. Thus, we take the isolated black holes to have the same velocity dispersion and scale height as black hole X-ray binaries.

### 2.3 Mass distribution of isolated black holes

The distribution of masses of black holes in X-ray binaries and microlensing events can be fit with a power law mass distribution,

$$dN/dM = n_M M^{-\gamma}, \tag{3}$$

with a lower mass cutoff at $M_1$ and upper mass cutoff of $M_2$. We obtain a best fit for $\gamma = 0.6$, $M_1 = 4{\rm M}_\odot$, and $M_2 = 14{\rm M}_\odot$ (Agol & Kamionkowski 2001). Since there may be larger-mass black holes that have not yet been detected, we impose an upper limit mass cutoff of $M_2 = 50{\rm M}_\odot$ based on the theoretical mass limit for pulsational stability (Schwarzchild & Härm 1959), assuming that about half of the mass is lost before collapse. This yields $M_1 = 4{\rm M}_\odot$ and $\gamma = 2.4$, close to the value of the Salpeter IMF (Agol & Kamionkowski 2001). The average mass of either distribution is $\sim 9{\rm M}_\odot$, close to the mean of the data $\langle M\rangle = 9.6 M_\odot$. We have normalized this to unity, $n_M = (\gamma-1)/(M_1^{1-\gamma} - M_2^{1-\gamma})$, and we assume that it applies throughout the Galaxy. We will later mention how our predictions differ for $M_2 = 13{\rm M}_\odot$, but will otherwise use $M_2 = 50{\rm M}_\odot$.

## 3 EFFICIENCY OF ACCRETION

### 3.1 Angular momentum of accreted material

The Bondi-Hoyle formula may be appropriate for computing the accretion rate, but not the efficiency. If the accreting gas were perfectly uniform, then the accreted angular momentum is quite small, and the accretion flow follows a one-dimensional supersonic solution, for which the luminosity can be predicted (Shapiro & Teukolsky 1983, Ipser & Price 1977). However, small perturbations in the density or velocity of the accreting gas will lead to an angular momentum large enough to circularise gas before it accretes (Shapiro & Lightman 1976). If there is a gradient in the density field that is perpendicular to the direction of motion of the black hole, then the accreted angular momentum scales as

$$l = \frac{1}{4}\frac{\Delta\rho}{\rho} v r_A, \tag{4}$$

where $\Delta\rho$ is the difference in velocity between the top and bottom of the accretion cylinder and $r_A = GM/(v^2+c_s^2)$ is the accretion radius. Numerical simulations confirm that this formula is correct to order of magnitude (Ruffert 1999). The observed density fluctuations in our galaxy scale as $\delta\rho/\rho \sim (L/10^{18}{\rm cm})^{1/3}$ (Armstrong, Rickett, & Spangler 1995), extending down to a scale of $\sim 10^8$ cm. The exponent of this scaling is nearly consistent with a Kolmogorov spectrum of density (Dubinski et al. 1995). Evaluating this at $L = 2r_A$, we can then find the radius of the resulting accretion disc, $r_{\rm disc}$, by equating the angular momentum of the gas with the Keplerian angular momentum due to the black hole, $l_{\rm Kep} = \sqrt{GMr_{\rm disc}}$. This gives

$$\frac{r_{\rm disc}}{r_g} = 10^4 r_g \left(\frac{M}{9{\rm M}_\odot}\right)^{2/3} \left(\frac{\sqrt{v^2+c_s^2}}{40{\rm km\ s}^{-1}}\right)^{-10/3}. \tag{5}$$

So, we see that a disc will almost always form in interstellar accretion. A similar argument is given in Fujita et al. (1998) for the case of molecular clouds, for which the slope of velocity fluctuations is similar to that expected by a Kolmogorov spectrum (Larson 1981). The neutral interstellar medium seems to follow a power-law with a similar slope (Lazarian & Pogosyan 2000), which will also lead to non-zero accreted angular momentum; however, the length scales probed in molecular and atomic gas are much larger than the scale of the accretion radius.

The accretion time scale for the disk scales as $t_d = \alpha_{SS}^{-1}(GM/r_{\rm disc}^3)^{-1/2}(r_{\rm disc}/h)^2$ where $h$ is the height of the disc and $\alpha_{SS}$ is the ratio of the viscous stress to the pressure in the disk. If the velocity and density fields of the ISM are incoherent on the scale of these fluctuations, then the angular momentum can change on a time scale of $t_a = r_A/v$ as gas will be accreted with the angular momentum vector pointing in a different direction after this time scale. Thus, the angular momentum of the disc can be reduced due to a random walk of the accreted angular momentum vector if $t_a \ll t_d$. We estimate

$$\frac{t_d}{t_a} \sim 2\frac{r_A}{2\times 10^{13}{\rm cm}}\left(\frac{0.1r}{h}\right)^2\left(\frac{\alpha_{SS}}{0.1}\right)^{-1}, \tag{6}$$

which indicates that there may only be a slight reduction in the angular momentum since these time scales are comparable. The residual angular momentum means that we *cannot* use spherical-accretion formulae for the luminosity, but we must estimate the efficiency of the accretion disc that forms.

### 3.2 Range of efficiencies

We assume that the black holes radiate a spectrum with spectral index $\alpha = 1$, where $F_\nu \propto \nu^{-\alpha}$, consistent with the typical spectrum of black-hole X-ray binaries, so that equal energy is emitted per unit decade of energy. We define $L_{\rm ion}$ as the luminosity from 1 to 1000 Ryd (13.6 eV), so the efficiency is $\epsilon_{\rm ion} = L_{\rm ion}/(\dot{M}c^2)$. Estimates of the accretion rate in Cygnus X-1 indicate that it is accreting with an X-ray efficiency of $\epsilon_{\rm ion} \sim 10^{-1}$ (Shapiro & Teukolsky 1983). However, at low accretion rates the density of the gas decreases, so it may not be able to cool, reducing the radiative efficiency. By estimating the mass accretion rates in black-hole X-ray binaries and X-ray luminosities in the quiescent state, Lasota (2000) concludes that the 2–10 keV efficiency is about $2\times 10^{-6}$ assuming that this luminosity is solely due to accretion, implying $\epsilon_{\rm ion} \sim 10^{-5}$. Low upper limits on the X-ray Bondi-accretion efficiencies are inferred for some supermassive black holes in elliptical galaxies (Loewenstein et al. 2001). The Galactic-centre black hole has an X-ray efficiency of $\sim 4\times 10^{-8} - 2\times 10^{-6}$ in the 2–10 keV band for a Bondi-Hoyle accretion rate of $10^{-6}{\rm M}_\odot$ yr$^{-1}$ (Baganoff et al. 2001). Thus, we parameterize our results in terms of an unknown X-ray efficiency.

For certain ranges of parameters, the disc may be unstable to the hydrogen-ionisation disc instability (Lasota 2001), creating intermittent outbursts of higher luminosity between long periods of quiescence, with changes in luminosity of $10^5$. We will discuss the possible effect this may have on the number of detectable sources in section 6.2.

### 3.3 Radiative feedback

The gas in the vicinity of the black hole will be heated by the ionising radiation field produced by accretion. If the temperature rises enough, then the accretion radius, and thus the accretion rate, will decrease (Shvartsman 1971, Ostriker et al. 1976). For an $\alpha = 1$ spectrum, the mean opacity from 1-1000 Ryd of neutral gas with cosmic abundance is $\sigma_{\rm cold} = 3.87\times 10^{-18}$ cm$^2$ per hydrogen atom. The heating rate is then given by $H = L_x n_H \sigma_{\rm cold}/(4\pi R^2)$, where $R$ is the distance from the black hole. For temperatures smaller than $\sim 10^4$ K and for a small ratio of radiation energy density to gas energy density, the heating rate greatly exceeds the cooling rate. Consider a fluid element directly in front of the path of a moving black hole. As the black hole approaches with velocity $v$, the ratio of the total heating rate to the initial energy density, $e_0$ of the gas is

$$\frac{e_{\rm tot}}{e_0} = \frac{1}{e_0}\int_R^\infty dRH/v = 2\times 10^5 \epsilon_{\rm ion} v_{40}^{-2}(r/r_A)T_4^{-1}, \tag{7}$$

where $e_{\rm tot}$ is the total energy density absorbed by a fluid element (neglecting cooling), $v = v_{40}40$km s$^{-1}$ and $T = T_4 10^4$ K. Thus, even for small efficiencies the gas is strongly heated outside the accretion radius. Once H and He are ionized, the mean opacity drops by three orders of magnitude, and the gas remains at around $2\times 10^4$ K. This has been confirmed with detailed numerical simulations by Blaes, Warren & Madau (1995). Above this temperature, the cooling and heating times become much longer than the accretion time so the gas falls in adiabatically. Thus we take the temperature of the accreted gas to be $T_0 = 2\times 10^4$ K for all phases of the ISM except the hot HII.

## 4 GAS IN OUR GALAXY

### 4.1 Phases of the ISM

The interstellar medium in our Galaxy consists of at least five identifiable phases (Bland-Hawthorn & Reynolds 2000) in approximate pressure equilibrium, $P \sim 2\times 10^3 k_B$. The highest accretion rates will occur in the regions of the highest density. This means that the observable sources will be dominated by the giant molecular clouds (GMCs) consisting mostly of $H_2$

($T \sim 10$ K) and the cold neutral medium consisting of HI clouds (CNM, $T \sim 10^2$ K). These phases comprise approximately 40 and 50 per cent of the total mass of gas in our Galaxy.

The warm neutral and ionised components ($T \sim 8000$K) of the interstellar medium have densities that are $\sim 10^{-2}$ of the CNM, so the maximum accretion rates are $\sim 10^{-2}$ times smaller than than the maximum for the CNM, while the hot component of the ISM ($T \sim 10^6$K) has a density $\sim 10^{-2}$ of the warm components, reducing the maximum accretion rate by another factor of $10^{-2}$. However, these phases fill a much larger volume in the interstellar medium, and thus should be considered.

We next refine the above estimates by considering the distribution of each phase as a function of number density.

### 4.2 Filling fraction of interstellar medium

To estimate the distribution of accretion rates for black holes in our Galaxy requires knowing the volume of the Galaxy filled by gas of a given number density. We define this as

$$\frac{df}{dn} = f_0 n^{-\beta}, \tag{8}$$

where $df/dn$ is the fraction of volume filled by gas with number density between $n$ and $n + dn$, and $f_0$ is a normalization constant. Berkhuijsen (1999) has shown that $\beta_{GMC} \sim 2.8$, while $\beta_{CNM} \sim 3.8$. This can be seen for the molecular clouds by noting that the mass function of molecular clouds in our Galaxy scales as $dN/dM \propto M^{-1.6}$ (Dickey & Garwood 1989), while number density of clouds scales with size, $D$, as $n \propto D^{-1}$ (Larson 1981, Scoville & Sanders 1987). Assuming that clouds have a spherical volume, one finds $df/dn \propto V(dM/dn)(dN/dM) \propto n^{-2.8}$. Since the number density-size relation is derived for the average density of clouds, $\beta$ may be slightly smaller since each cloud may contain regions where the gas density is higher than average.

We assume that the GMCs span number densities from $n_1 = 10^2$ to $n_2 = 10^5$ cm$^{-3}$, while the CNM spans number densities from $n_1 = 10$ to $n_2 = 10^2$ cm$^{-3}$. Finally, we assume that the scale height of the molecular clouds is 75 pc, while the scale height of the CNM is 150 pc.

The surface mass density of molecular gas as a function of radius we take from Clemens, Sanders & Scoville (1988) and Scoville & Sanders (1987), while the distribution of the CNM we assume is constant with $\Sigma = 4.5$M$_\odot$ pc$^{-2}$ for $R > 4$ kpc, and zero inside 4 kpc (Scoville & Sanders 1987). The molecular-gas surface density has a a strong peak at the Galactic centre, another peak around 5 kpc from the Galactic centre, then decreases outwards (Scoville & Sanders 1987). We ignore variations of the surface density in azimuth, and we approximate the distribution in $z$ as an exponential, $f_0(z) = f_0(0)\exp(-|z|/H)$. From these surface densities, we compute the filling fraction in the mid-plane as,

$$f_0(0) = \frac{\Sigma(\beta-2)(n_1^{1-\beta} - n_2^{1-\beta})}{2H\mu(\beta-1)(n_1^{2-\beta} - n_2^{2-\beta})}, \tag{9}$$

where $\mu = 2.72 m_p$ for the GMC, and $\mu = 1.36 m_p$ for the CNM. At the solar circle, this gives $f_0(\mathrm{GMC}) = 10^{-3}$, while $f_0(\mathrm{CNM}) = 0.04$.

The warm HI, warm HII, and hot HII we take as constant densities of 0.3, 0.15, and 0.002 cm$^{-3}$ respectively, mid-plane filling factors of 35, 20, and 40 per cent, as well as scale heights of 0.5, 1, and 3 kpc (Bland-Hawthorn & Reynolds 2000). We assume that the hot HII has a temperature of $10^6$ K, and thus $c_s = 150$ km s$^{-1}$. The corresponding surface mass densities are 4, 2, and 0.2 M$_\odot$ pc$^{-2}$, respectively, which we assume are constant as a function of Galactic radius.

## 5 ACCRETION RATE AND LUMINOSITY DISTRIBUTION FUNCTIONS

The distribution function of mass-accretion rate for black holes located at a given region in the Galaxy is given by

$$\frac{d^2N}{d\dot{M}dV} = \int_{M_1}^{M_2} dM \int_{n_1}^{n_2} dn \int_0^\infty dv \frac{df}{dn}\frac{d^2n_{\mathrm{BH}}}{dMdv}\delta(\dot{M}(n,M,v) - \dot{M}), \tag{10}$$

where $dV$ is the volume element and

$$\frac{d^2n_{\mathrm{BH}}}{dMdv} = N_{\mathrm{BH}}(R,z)\sqrt{\frac{2}{\pi}}\frac{v^2}{\sigma_v^3}\exp\left[-\frac{v^2}{2\sigma_v^2}\right] n_M M^{-\gamma}. \tag{11}$$

We define $\dot{M}_0 = \pi G^2 \mathrm{M}_\odot^2 m_p (1\mathrm{km\ s^{-1}})^{-3} = 3.8\times10^{14}$, so that $\dot{M}(n,M,v) = \dot{M}_0 n M^2 (v^2 + c_s^2)^{-3/2}$. For a given mass and sound speed, we can define the minimum number density required for accretion at a rate greater than $\dot{M}$: $n > n_0 = \dot{M}c_s^3/(\dot{M}_0 M^2)$. Using equations (1) and (3), we can first carry out the $v$ integration analytically,

$$\frac{d^2N}{d\dot{M}dV} = N_{\mathrm{BH}} \int_{M_1}^{M_2} dM\, n_M M^{-\gamma} \int_{\max\{n_1,n_0\}}^{\max\{n_2,n_0\}} dn f_0 n^{-\beta} \sqrt{\frac{2}{\pi}}\frac{v_0}{\sigma_v^3}\frac{(\dot{M}_0 n M^2)^{2/3}}{\dot{M}^{5/3}}\exp\left[-\frac{v_0^2}{2\sigma_v^2}\right], \tag{12}$$

where $v_0^2 = (\dot{M}_0 n M^2/\dot{M})^{2/3} - c_s^2$. The remaining two integrals we compute numerically.

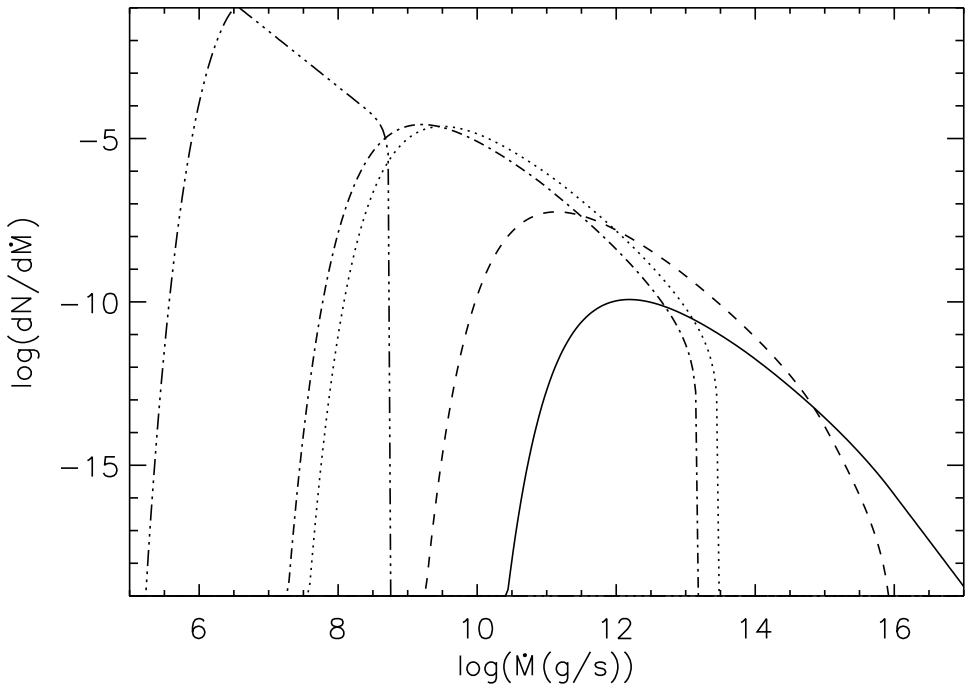


Fig. 1: The number density of black holes accreting with accretion rates between $\dot{M}$ and $\dot{M} + d\dot{M}$ as a function of $\dot{M}$ at the solar radius for $\sigma_v = 40$ km s$^{-1}$. The solid curve refers to black holes accreting within molecular clouds, while the short dashed curve refers to black holes within the cold neutral medium. The dotted curve is black holes within the warm HI, the dash-dot curve for the warm HII, while the dash-triple dot curve for the hot HII.

In Figure 1 we plot the function $dN/d\dot{M}$ for the various phases of the interstellar medium at the solar circle. The densest gas (GMCs) dominates the highest accretion rates, while the hottest gas dominates the lowest accretion rates. For the hot HII, accretion is subsonic and $n$ is assumed to be constant, so $\dot{M} \propto M^2$. Thus, $dN/d\dot{M} \propto \dot{M}^{-(1+\gamma)/2}$, spanning a range in $\dot{M}$ of $(M_2/M_1)^2$, or two decades. This is consistent with the numerical spectrum shown in Figure 1. The other phases have more complicated accretion-rate distributions since $\sigma_v > c_s$.

To compute the expected total number of black holes in the Galaxy accreting at a rate $\dot{M}$, we integrate the luminosity functions (assumed to be constant) over the gas filling fraction times the number density of black holes as a function of position over the entire Galaxy,

$$\frac{dN}{d\dot{M}} = \left.\frac{d^2N}{d\dot{M}dV}\right|_{(R_\odot, z=0)} \int_0^\infty dR\, 2\pi R \exp\left[-\frac{R-R_\odot}{R_{\rm disc}}\right] 2\frac{\Sigma(R)}{\Sigma(R_\odot)} \int_0^\infty dz \exp\left[-\frac{z}{H_{\rm BH}} - \frac{z}{H_{gas}}\right]. \quad (13)$$

Figure 2(a) shows $N(>\dot{M}) = \int_{\dot{M}}^\infty d\dot{M}'(dN/d\dot{M}')$ for both black holes and neutron stars. For neutron stars, we choose $M = 1.4{\rm M}_\odot$, 86 per cent with $\sigma_v = 175$ km s$^{-1}$ and 14 per cent with $\sigma_v = 700$ km s$^{-1}$ (Cordes & Chernoff 1998), $N_\odot = 5.2 \times 10^5$ kpc$^{-3}$, and $H = 1$ kpc, yielding a total of $10^9$ neutron stars within our galaxy. The total number of accreting black holes is smaller than the total number in the disk since we have assumed that the gas filling factor decreases with scale height. This reduction may be artificial since gas at some density presumably fills the entire Galaxy, but this only affects small accretion rates.

We expect $\sim 10^4 N_9$ isolated black holes to be accreting at rates comparable to the estimated rates in black-hole X-ray binaries, $\dot{M} > 10^{15}$ g s$^{-1}$ (van Paradijs 1996). This exceeds the parent population of black-hole X-ray binaries, which may be $10^{2-3}$ (Iben et al. 1995). Black holes outnumber neutron stars due to their larger mass and smaller space velocity as shown in Figure 2(a).

To compute the number of detectable isolated black holes requires converting the accretion-rate distribution into a luminosity function. Given the uncertainties in accretion physics, we will make two assumptions based on what is known about black-hole X-ray binaries: persistent and transient sources. The first assumption shown in Figure 2(b) is that the sources are time-steady, similar to high-mass X-ray binaries such as Cygnus X-1. Under this assumption, we simply convert the accretion rate into an X-ray luminosity in a given X-ray band. Shown is the ionising radiation band from 1–1000 Ryd for $\epsilon_{\rm ion} = 10^{-5}$; the horizontal axis simply scales with efficiency. The black-hole and neutron-star functions overlap for $\epsilon_{\rm ion} \sim 10^{-5}$ despite the lower black-hole efficiency due to the larger black-hole mass, smaller velocity dispersion, and smaller scale height. The total luminosity of isolated accreting black holes within the Milky Way is $\sim 10^{36} N_9 \epsilon_{-5}$ erg s$^{-1}$.

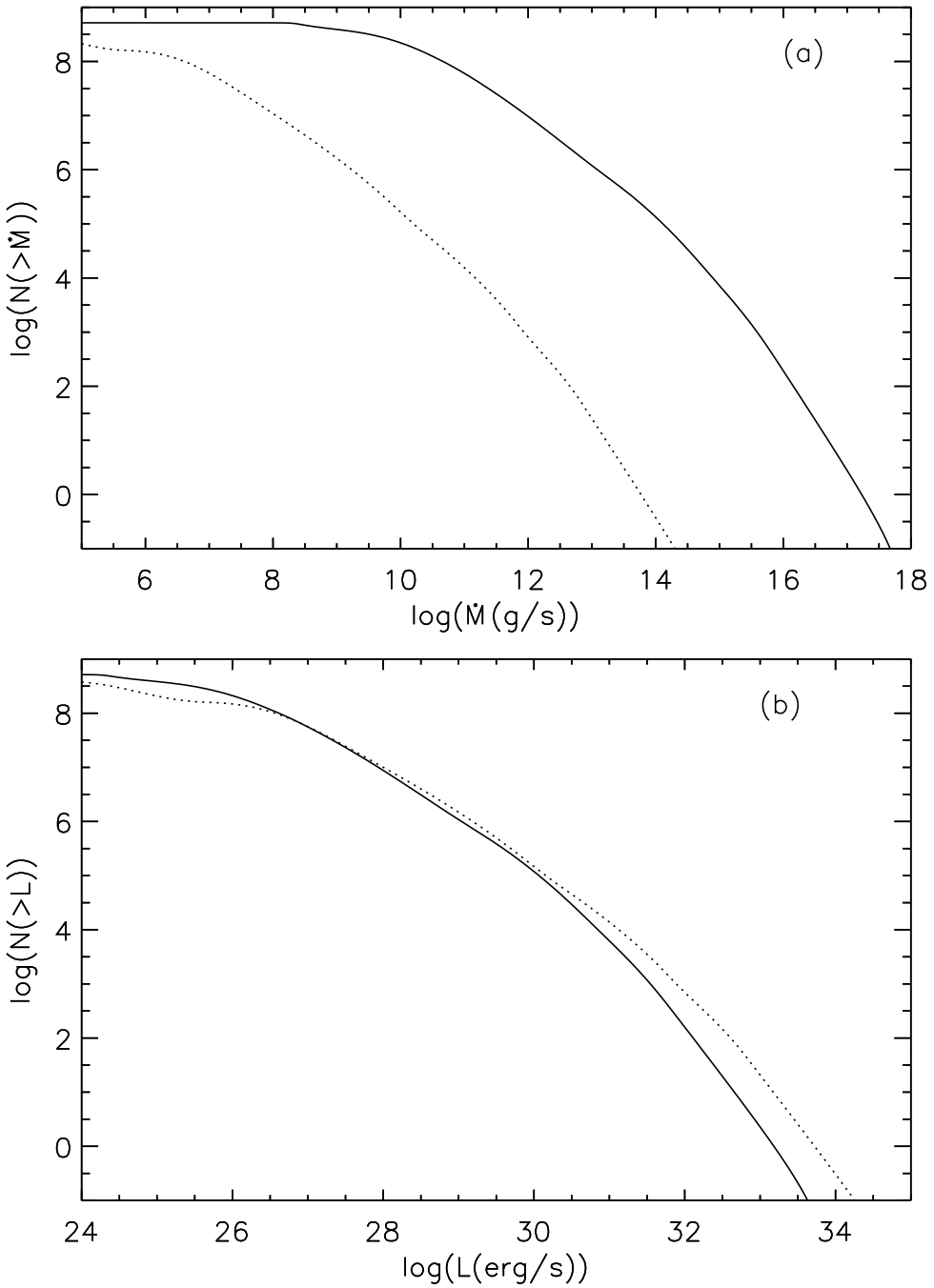


Fig. 2: (a) The number of black holes in the Milky Way with accretion rates greater than $\dot{M}$ for $\sigma_v = 40$ km s$^{-1}$ (solid line). For comparison, the dotted line shows the same computation for neutron stars. (b) The number of black holes in the Milky Way with luminosities greater than $L_{\rm ion}$ with $\epsilon_{\rm ion} = 10^{-5}$ and the number of neutron stars for $\epsilon_{\rm ion} = 10^{-1}$ (dotted line).

The second assumption that the black holes are transient we discuss in section 6.2 below.

## 6 DETECTION PROBABILITY

To compute the detection probability, we need to integrate the number of sources above a given observed flux as a function of position within the Galaxy. We will consider two energy emission bands, 'soft' X-ray from 1–10 keV, and 'hard' X-ray from 10–100 keV, which have efficiencies of $\epsilon_{\rm soft}$ and $\epsilon_{\rm hard}$. Since the model spectrum we have used is flat, $\nu f_\nu \propto \nu^0$, the luminosity per unit decade of photon energy is constant. Thus, the flux in each of these bands is 1/3 of the flux of ionising photons which

covers three decades, or $\epsilon_{\rm soft} = \epsilon_{\rm hard} = \epsilon_{\rm ion}/3$. A more complex X-ray spectrum will change our results by factors of order unity, which we defer to future work given the poor theoretical understanding of the spectra of accreting black holes.

For neutron stars, we assume a spectrum composed of a blackbody with $T = 0.15$ keV plus a power law with $\alpha = 1$ (i.e. flat in $\nu F_\nu$) and the flux from 1–10 keV equal to 1 per cent of the total flux of the blackbody component. This was chosen to be similar to the spectra of neutron-star binaries Cen X-4 and Aquila X-1 in quiescence (Rutledge et al. 2001a,b). This spectrum yields $\epsilon_{\rm soft} = 0.13\epsilon_{\rm ion}$ and $\epsilon_{\rm hard} = 0.03\epsilon_{\rm ion}$ due to the fact that most of the flux is in the extreme ultraviolet. We neglect photoelectric absorption since the half-column density of molecular clouds is approximately $N_H \sim 1 \times 10^{22}{\rm cm}^{-2}$, which leads to absorption of only 36 per cent of the flux in the soft X-ray band (using the opacities of Morrison & McCammon 1987). Toward the Galactic centre, the hydrogen column density is about $N_H \sim 6 \times 10^{22}{\rm cm}^{-2}$ due to the ring of gas near the centre, leading to absorption of about 86 per cent of the soft flux. In the hard–X-ray band, the absorption is negligible.

### 6.1 Persistent sources

For the persistent-source assumption, we assume that the accretion flow emits isotropically, so we simply need to integrate the luminosity function over the entire galaxy with the transformation:

$$\frac{dN}{dFdV} = \frac{dN}{d\dot{M}dV}\frac{4\pi D^2}{\epsilon_{\rm soft,hard}c^2}, \tag{14}$$

where $D$ is the distance to a given point in the Galaxy. Figure 3 shows the predicted number of sources as a function of flux integrated over the entire Galaxy for the persistent-source assumption. Despite the much lower assumed efficiency, the number of detectable black holes becomes comparable to the number of detectable neutron stars for $\epsilon_{BH} \sim 10^{-4}\epsilon_{NS}(N_{BH}/N_{NS})^{0.8}$. The number of black holes above a certain flux at high flux scales approximately as $N(>F) = 10^4 F^{-1.2}$ near $F = 10^{-15}\epsilon_{-5}$ erg cm$^{-2}$ s$^{-1}$. Given the flatness of this dependence, the best detection strategy is to cover as much area of the sky as possible, assuming the constraint of a fixed amount of observing time with an X-ray telescope with a sensitivity that scales as $t^{-1/2}$. Reducing the mass cutoff from $M_2 = 50{\rm M}_\odot$ to $M_2 = 13{\rm M}_\odot$ only decreases the number of objects by a factor of $\sim 2$ since there are fewer objects at high mass (Figure 3).

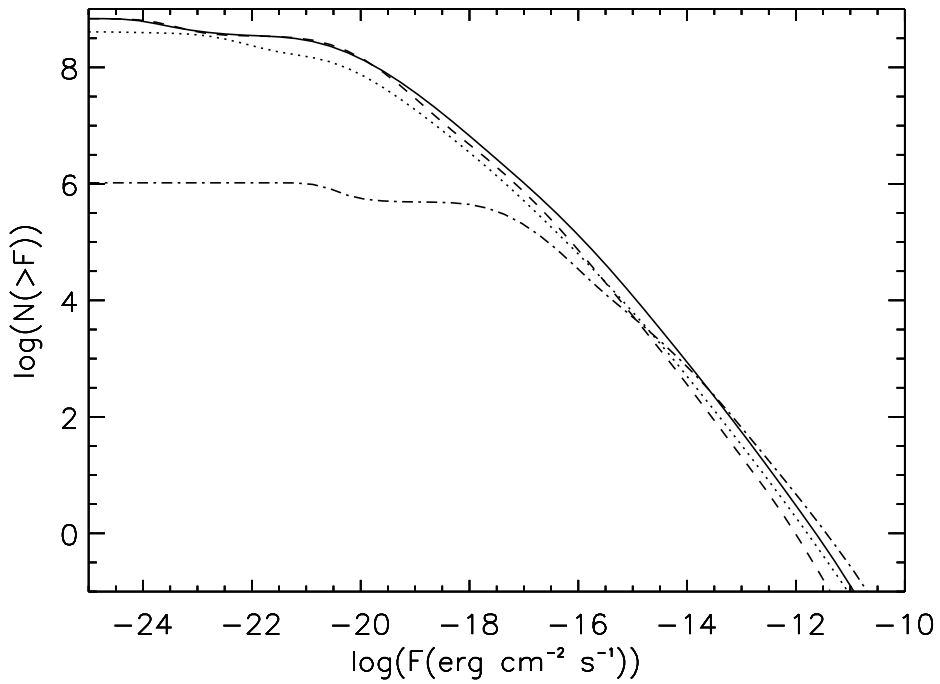


Fig. 3: The number of black holes visible to an observer located within the Solar system as a function of X-ray flux in either the soft or hard X-ray bands for a persistent accretion efficiency of $\epsilon_{\rm ion} = 10^{-5}$ with $\epsilon_{\rm soft,hard} = \epsilon_{\rm ion}/3$ for $M_2 = 50{\rm M}_\odot$ (solid line) and $M_2 = 13{\rm M}_\odot$ (dashed line). For comparison the number of neutron stars above a given soft X-ray flux is shown as well in the soft X-ray band with $\epsilon_{\rm soft} = 0.13\epsilon_{\rm ion} = 0.013$ (dotted line). In addition, we show predictions for a population of $10^6$ black holes with mass $250{\rm M}_\odot$ for efficiencies of $10^{-5}$ (dash-dot line). Note that the horizontal axis scales with efficiency for each object.

We have also computed the the number density of black holes with fluxes greater than $10^{-15}\epsilon_{-5}$ erg cm$^{-2}$ s$^{-1}$ as a function of Galactic latitude and longitude for one quadrant of the Galaxy (Figure 4). The black holes are strongly concentrated toward the Galactic plane and toward the Galactic centre. Half of the black holes lie within the dashed contour which covers an area of 504 deg$^2$ in Figure 4, giving an average of $3N_9$ per square degree within this region near the Galactic plane. We have not

attempted to include the inhomogeneity of the ISM which might be important for nearby black holes in the local bubble or for black holes in interstellar clouds.

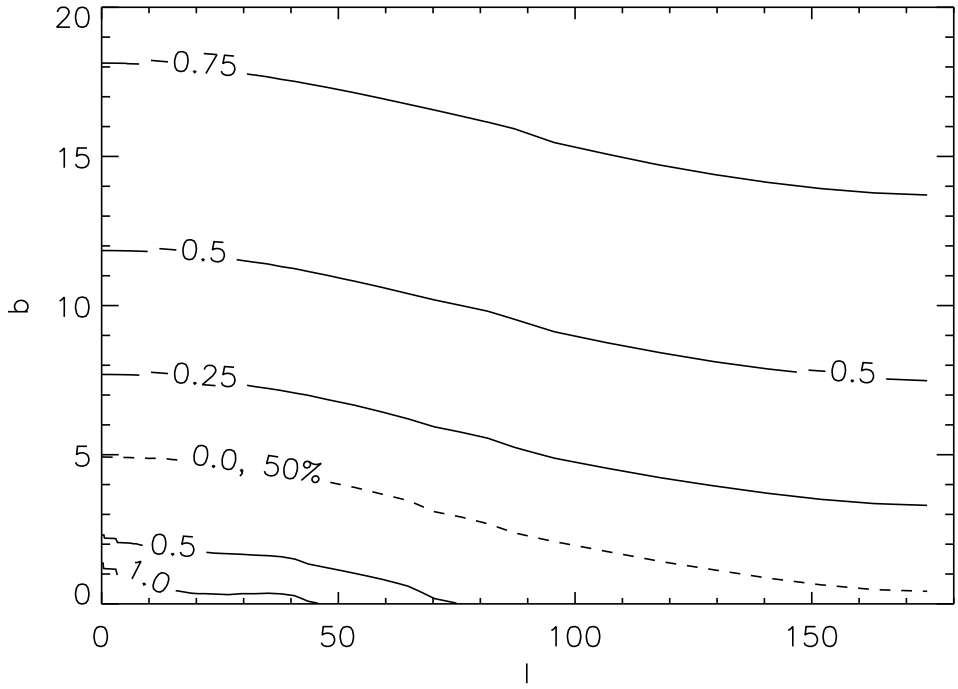


Fig. 4: The logarithm of the number density of black holes per degree square with fluxes above $F_X = 10^{-15}\epsilon_{-5}$ erg cm$^{-2}$ s$^{-1}$ in the soft or hard band as a function of galactic longitude, $l(^\circ)$, and latitude, $b(^\circ)$. The labels indicate the logarithm of the number density. The dashed line indicates the contour within which 50 per cent of the black holes are contained. The total number of black holes above this flux level is $\sim 5000$, while the maximum number density is 94 per square degree at the Galactic Center.

Finally, we have computed the distribution of sources with distance from the Sun. Figure 5 shows the number of black-hole sources with fluxes greater than $F = 10^{-15}\epsilon_{-5}$ erg cm$^{-2}$ s$^{-1}$ less than a given distance for each of the phases of the ISM. The total number of sources above this flux level is $3800N_9$ in the GMCs, $6700N_9$ in the CNM, $900N_9$ in the warm HI, $200N_9$ in the warm HII, and 0 in the hot HII. The average distance for the detectable black holes is 5 kpc in the GMCs, 1 kpc in the CNM, 200 pc in the warm HI, and 140 pc in the warm HII. The average distance of black holes in all phases is 2 kpc. Note that there is a rise in the number of black holes in GMCs at the Galactic centre (8 kpc away) since the surface density of molecular gas increases by a factor of $\sim 10$ within 500 pc of the Galactic centre. The sources in the gas clouds tend to be more distant since it requires looking further in the Galaxy to find clouds, while the the sources in the interstellar gas tend to be closer since they are fainter due to lower accretion rates.

The sensitivity of the ROSAT All-Sky Survey (RASS) Bright Source Catalog is about $10^{-12}$ erg cm$^{-2}$ s$^{-1}$ (Voges et al. 1999; we have converted count rate to flux assuming $\alpha = 1$), so at most $3N_9\epsilon_{-5}^{1.2}$ accreting black hole should have been detected by this survey given the assumption of persistence. We can see immediately from Figure 3 why it may have been difficult to detect isolated accreting neutron stars with the RASS since we predict about one visible neutron star on the sky at this flux level, which will be reduced further by X-ray absorption. Danner (1998) has surveyed sources in molecular clouds within the RASS, finding no new isolated neutron-star candidates, and thus, we presume, no isolated black-hole candidates. For an X-ray observatory such as *EXIST*, which will reach sensitivities of $\sim 10^{-13}$ erg cm$^{-2}$ s$^{-1}$ for one-year co-added data (Grindlay et al. 1999 ), about $\sim 50N_9\epsilon_{-5}^{1.2}$ sources may be detectable at hard X-ray energies as well. *EXIST* will have an angular resolution of about 2 arcminutes and position sensitivity of $\sim 30$ arcsec, which should make identification feasible within molecular clouds.

The *Chandra* and *XMM-Newton* observatories have much better sensitivities $\sim 10^{-14}$ erg cm$^{-2}$ s$^{-1}$ for a 10 kilo-second (ksec) observation; however, both satellites cover a much smaller field of view ($16' \times 16'$). The ChaMPlane survey (*Chandra* Multi-wavelength Galactic Plane Survey, Wilkes et al. 2000) will cover about 1 square degree per year to a flux of $\sim 10^{-15}$ erg cm$^{-2}$ s$^{-1}$ for the 1–10 keV band. This flux limit is deep enough that $\sim 10^4 N_9\epsilon_{-5}^{1.2}$ sources within the Galactic plane might be detectable (Figure 3); however, the central 50 per cent are spread over an area of 504 deg$^2$ in the Galactic Plane (Figure 4). The *XMM-Newton* serendipitous Survey will cover an area of the sky $\sim 10$ times larger than the *Chandra* Serendipitous Survey at similar sensitivity (Watson et al. 2001). Thus, these surveys may result in $\sim 30N_9\epsilon_{-5}^{1.2}$ detections per year.

One might expect that targeting molecular clouds may be advantageous for finding black holes. However, due to their proximity, the 23 clouds within 1 kpc have angular sizes of about 5–20° (Dame et al. 1987), which will make them rather difficult to cover with the small field of view of *Chandra* or *XMM-Newton*. For instance, the single pointing in the $\rho$-Ophiucus molecular cloud observed by Imanishi et al. (2001) covers a volume $\sim 18$ pc$^3$ (assuming the cloud is spherical), so we expect

only $\sim 3 \times 10^{-2} N_9$ black holes to reside within the observed volume. Observations pointed at molecular clouds will not improve these detection rates, but observations pointing toward the Galactic centre should improve the number of detections significantly. Surveys targeted at the Galactic Center (Baganoff et al. 2001) may find $7 N_9 \epsilon_{-5}^{1.2}$ per *Chandra* or *XMM-Newton* field.

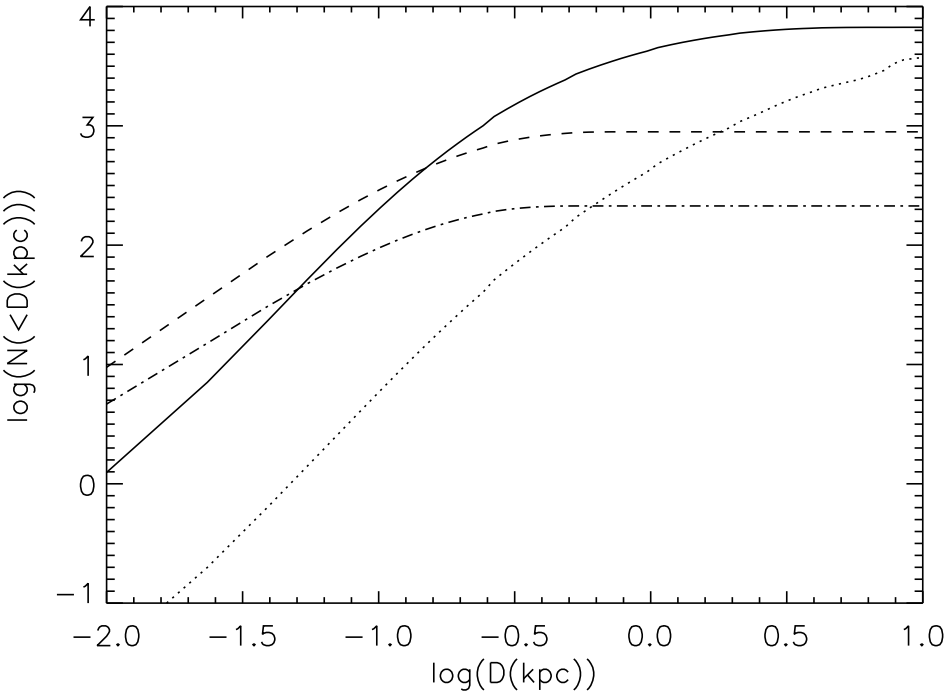


Fig. 5: The total number of black hole sources with fluxes greater than $F = 10^{-15} \epsilon_{-5}$ erg cm$^{-2}$ s$^{-1}$ and less distant than $D$. The solid line is for the CNM, the dotted line for the GMCs, the dashed line for the warm HI, and the dash-dot line for the warm HII.

### 6.2 Transient sources

The second assumption is that each of the sources are transient, driven by the hydrogen-ionisation instability at radii in the accretion disc with $T \sim 5000$ K as in low-mass X-ray binaries. In this case, we assume that the sources undergo outbursts for several months with luminosities near Eddington, while remaining faint for several decades. Chen, Shrader & Livio (1997) have shown that soft X-ray transients tend to peak at $L_{\rm out} \sim 0.2 L_{\rm Edd}$ with an average duration (decay time scale) of $t_o \sim 20$ days and recurrence times varying from 2 years to 60 years for black holes. These are only the observed transients; transients with longer recurrence time scales may not have had time to repeat. If we assume that each black hole accretes quiescently for a time $t_q$, storing up mass in the accretion disk with a small fraction of gas accreting on to the black hole, and then all of this mass is released in an outburst of duration $t_o$, then

$$t_q = 130 yr \frac{L_{\rm out}}{0.2 L_{\rm Edd}} \frac{t_o}{20 {\rm days}} \left( \frac{\epsilon_o \dot{M}}{10^{14} {\rm g\ s^{-1}}} \right)^{-1} \frac{M}{9 {\rm M}_\odot}, \tag{15}$$

where $\epsilon_o$ is the radiative efficiency of accretion during outburst. The outburst rate in the Milky Way is then

$$\dot{N}_{\rm out} = \int_{M_1}^{M_2} dM \int_0^\infty d\dot{M} \frac{d^2 N}{dM d\dot{M}} t_q^{-1}. \tag{16}$$

Assuming a 10 per cent efficiency during outburst, we find $\dot{N}_{\rm out} \sim 536 N_9$ yr$^{-1}$ for $\sigma_v = 40$ km s$^{-1}$. This is clearly inconsistent with observations, demonstrating that not all isolated black holes undergo transient outbursts if the assumptions of our calculation are correct. If only black holes accreting above $\dot{M} > 10^{15}$ g s$^{-1}$ undergo outbursts, consistent with the observed X-ray novae (van Paradijs 1996), then these numbers reduce to 50 yr$^{-1}$, still large given that about $\sim 1$ transient is detected each year, and generally they are found to have companions. We conclude that only a small fraction of isolated black holes might experience transience similar to X-ray novae.

### 6.3 Detecting microlensing candidates

The uncertainty in distance of the MACHO black-hole microlensing candidates leads to an uncertainty in their mass, and thus an uncertainty in their status as black holes. One possible way to constrain the mass of these lenses is to look for X-rays from

accretion. Figure 6 shows the flux as a function of distance for MACHO 96-BLG-5, MACHO 98-BLG-6, and OGLE-1999-BUL-32 (Mao et al. 2001) for a number density of 1 cm$^{-3}$ with the total velocity set to $\sqrt{3/2}$ times the observed sky velocity projected on to the lens plane (ignoring the unknown projected source velocity) and subtracted from the Galactic rotation velocity (220 km s$^{-1}$) and an X-ray efficiency of $\epsilon_{\rm ion} = 10^{-3}$. We note that if the sky velocity of the source is significant, then the inferred lens velocity will be different, typically smaller, which will increase the luminosity. The flux scales as $F \propto \epsilon n D^{-4}$ for small distances since the mass depends on the inverse of the distance and the flux decreases as the inverse of distance squared. Observing in the X-ray would be advantageous to avoid confusion with the background microlensed star. In the soft X-ray, a 1–10 keV flux of $\sim 10^{-15}$ erg cm$^{-2}$ s$^{-1}$ can be detected with a $\sim 400$ ksec exposure with *Chandra* or $\sim 200$ ksec with *XMM-Newton*. A detection of a black-hole candidate at such a flux level will allow an upper limit on the distance of $\sim 1-3$ kpc to be placed, assuming they accrete from the diffuse ISM with $n < n_{\rm max} = 1$ cm$^{-3}$ and assuming an X-ray efficiency less than $\epsilon_{\rm max} = 10^{-3}$. A decrease in efficiency will lead to a decrease in flux, and thus a decrease in the distance upper limit. An upper limit on distance converts into a lower limit on mass, since $M \propto D^{-1}$, which may confirm the black-hole hypothesis. The mass lower limit is proportional to $M_{\rm min} \propto (\epsilon_{\rm max} n_{\rm max}/F)^{-1/4}$, a weak dependence on our assumed parameters. A cloud or companion could increase the accretion rate, resulting in a higher luminosity, thus a larger distance for the same flux; however, clouds occupy less than 5 per cent of the volume near the Galactic plane and can be searched for in HI 21 cm or CO absorption or emission (the MACHO fields are toward Baade's window, thus unlikely to contain a high molecular column density), while companions should be detectable with HST.

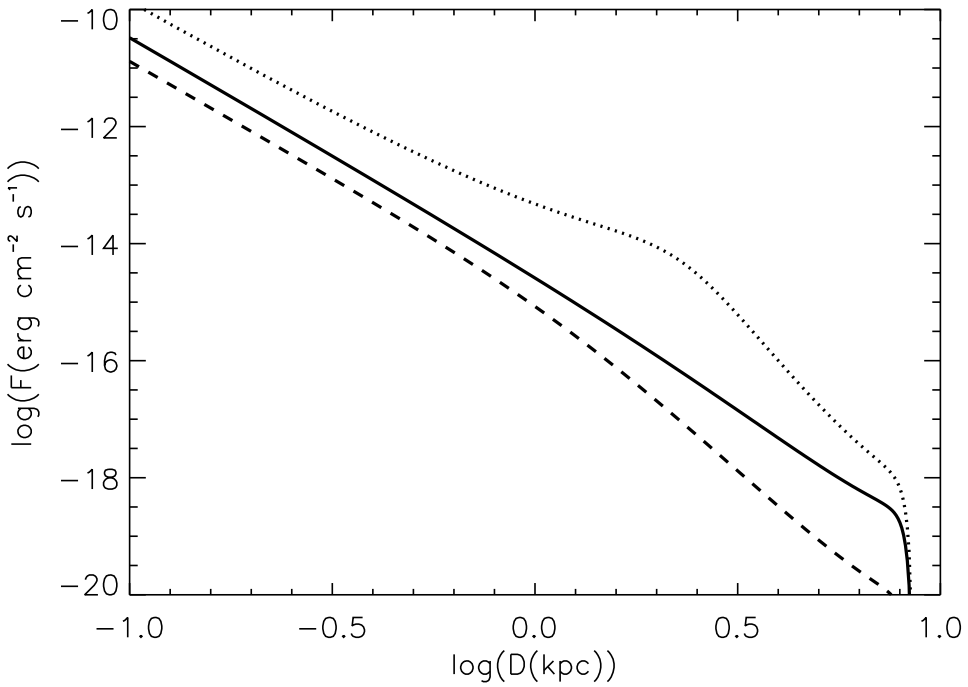


Fig. 6: The flux as a function of distance for MACHO 96-BLG-5 (solid), MACHO 98-BLG-6 (dashed) and OGLE-1999-BUL-32 (dotted) as a function of distance for $\epsilon_{\rm ion} = 10^{-3}$.

## 7 CONCLUSIONS

We have estimated the number of isolated black holes that might be revealed by their X-ray emission from accretion of interstellar gas. We have improved upon previous calculations by taking into account the density distribution of the interstellar medium, as well as using the known properties of black-hole X-ray binaries and MACHO black-hole candidates to constrain the phase space and accretion efficiency of isolated accreting black holes. We conclude that persistent isolated black holes may be competitive with neutron stars in creating detectable X-ray flux if their efficiencies differ by $\epsilon_{BH} \sim 10^{-4} \epsilon_{NS} (N_{BH}/N_{NS})^{0.8}$. The ROSAT survey did not have the sensitivity to detect either isolated accreting neutron stars or black holes; an all-sky survey with two orders of magnitude more sensitivity, $\sim 10^{-14}$ erg cm$^{-2}$ s$^{-1}$ dex$-1$, may be able to detect $\sim 10^3 N_9 \epsilon_{-5}^{1.2}$ accreting black holes. The X-ray observatories *XMM-Newton* and *Chandra* may be able to detect this population with pointed observations; however, they suffer from having small fields of view. Despite this limitation, Galactic plane surveys being carried out with these telescopes may be able to detect tens per year for $\epsilon_{-5} = 1$. If the accreting sources with $\dot{M} > 10^{15}$ g s$^{-1}$ go through transient outbursts, then 50 isolated black holes per year would be detectable as X-ray novae, so we reject this possibility since isolated X-ray novae have not been observed.

The greatest uncertainty in our predictions is the efficiency of black-hole accretion, with which we have parameterized our results. Most of the detectable black holes should reside in interstellar clouds that have higher densities; however, this

leads to the problem of confusion with other X-ray sources such as the coronae of massive stars. Some tests for whether an accreting object is a black hole are the following: 1) Is there high-energy emission? Accreting black holes tend to show spectra which have power laws extending up to $\sim 10^2$ keV (Grove et al. 1998). 2) What is the nature of the variability? Accreting black holes show no pulsations, show only QPOs with $\nu < 1$ kHz, and show power spectra that cut off around 500 Hz (Sunyaev & Revnivtsev 2000). 3) What is the mass? Without a binary companion, the mass of an accreting object is difficult to measure; however, this might be achieved by carrying out astrometry of background stars to look for gravitational distortion by the accreting object (Paczyński 2001). 4) What do other parts of the spectra look like? Accreting black holes can produce relativistic radio jets (Mirabel & Rodríguez 1999), and photoionisation of the surrounding gas might result in observable infrared lines (Maloney, Colgan & Hollenbach 1997).

There are several assumptions in our calculation that might affect the results. We have assumed that the accretion flow is one-dimensional, and that the sonic point is at the accretion radius. We have also assumed that the accretion is time steady; this may not be the case for higher accretion rates than we find for black holes accreting from the ISM (e.g. Grindlay 1978). If the black hole is moving slower than the sound speed at the accretion radius then the preheated region outside the accretion radius may have a chance to expand into the ISM, reducing the number density, and thus reducing the accretion rate. We have neglected mechanical feedback, which may occur if a jet or wind is developed. Recent work on non-radiating accretion flows indicates that strong winds can be formed which carry the bulk of the energy outwards as mechanical rather than radiative energy (Blandford & Begelman 1999, Igumenshchev, Abramowicz & Narayan 2000, Hawley, Balbus & Stone 2001). These authors argue that the accretion rate scales as $\dot{M} \propto r$. If the outer radius is taken as $r_A$, then $\dot{M}(10r_g) \sim 10(v/c)^2\dot{M}(r_A) \sim 2\times10^{-7}v_{40}^{-2}\dot{M}(r_A)$. If the outer radius is taken to be the circularization radius, then $\dot{M}(10r_g) \sim 10^{-3}(M/9\mathrm{M}_\odot)^{-2/3}[(v^2+c_s^2)^{1/2}/40\mathrm{km\ s}^{-1}]^{-10/3}$. Either of these circumstances will make black holes less visible, which in the formalism of this paper corresponds to a further reduction in the accretion efficiency. Magnetic fields will likely play an important role as they are amplified by flux-freezing, possibly heating the gas to virial temperatures (Igumenshchev & Narayan 2001) and can transport angular momentum via the magnetorotational instability once the circularization radius is reached, modifying the dynamics of the accretion flow. We have not explored the dependence of the efficiency on other parameters, which may result, for example, from changes in the gas density and angular momentum as a function of the accretion rate, so our extrapolation from estimated efficiencies of black-hole X-ray binaries may be too optimistic. The validity of these assumptions can be tested with 3-D radiation MHD simulations of a black hole accreting from an inhomogeneous medium, a daunting numerical problem.

It is possible that a population of intermediate-mass black holes (IMBHs) exist with larger masses around $250\mathrm{M}_\odot$, the remnants of the first generation of star formation (Madau & Rees 2001). The larger masses of these objects would result in yet larger accretion rates and luminosities by a factor of $\sim 10^3$, if they are distributed with same phase-space distribution as $9\mathrm{M}_\odot$ black holes. If we assume that $\sim 10^6$ IMBHs reside in our galaxy, then we find that the number of detectable objects at high fluxes may comparable to $9\mathrm{M}_\odot$ black holes accreting at the same efficiency (Figure 3). However, if these objects reside in the halo or bulge of the galaxy, the number detectable will be decreased significantly.

## ACKNOWLEDGMENTS

We acknowledge D. Bennett, L. Bildsten, O. Blaes, R. Blandford, J. Carpenter, D. Chernoff, G. Dubus, A. Esin, C. Fryer, J. Grindlay, T. Kallman, L. Koopmans, J. Krolik, Y. Lithwick, A. Melatos, S. Phinney, M. Rees, R. Rutledge, N. Scoville, and K. Sheth for useful conversations and ideas which greatly improved this work. This work was supported in part by NSF AST-0096023, NASA NAG5-8506, and DoE DE-FG03-92-ER40701. Support for the work done by EA was provided by the National Aeronautics and Space Administration through Chandra Postdoctoral Fellowship Award Number PF0-10013 issued by the Chandra X-ray Observatory Center, which is operated by the Smithsonian Astrophysical Observatory for and on behalf of the National Aeronautics Space Administration under contract NAS8-39073.

## REFERENCES

Alcock C. et al. (the MACHO collaboration), 2000, ApJ, 541, 734
Armstrong, J. W., Rickett, B. J., Spangler, S. R., 1995, ApJ, 443, 209
Baganoff, F. K. et al., 2001, Nature, 413, 45
Bailyn C. D., Jain R. K., Coppi P., Orosz J. A., 1998, ApJ, 499, 367
Bennett D. P. et al., 2001, submitted, astro-ph/0109467
Berkhuijsen, E. M., 1999, Plasma Turbulence and Energetic Particles in Astrophysics, Ostrowski, M. & Schlickeiser, R., eds., Kraków
Bildsten, L., Rutledge, R. E., 2000, ApJ, 541, 908
Blaes O. M., Madau P., 1993, ApJ, 403, 690
Blaes O., Warren O., Madau P., 1995, ApJ, 454, 370
Bland-Hawthorn J., Reynolds R., 2000, in Encyclopedia of Astronomy & Astrophysics, MacMillan and Institute of Physics Publishing
Blandford R. D., Begelman M. C., 1999, MNRAS, 303, L1
Bondi H., Hoyle F., 1944, MNRAS, 104, 273
Brandt W. N., Podsiadlowski Ph., Sigurdsson S., 1995, MNRAS, 277, L35
Campana S., Pardi M. C., 1993, A&A, 277, 477
Carr B. J., 1979, MNRAS, 189, 123

Chen W., Shrader C. R., Livio M., 1997, ApJ, 491, 312
Clemens D. P., Sanders D. B., Scoville N. Z., 1988, ApJ, 327, 139
Cordes, J. M., Chernoff, D. F., 1998, ApJ, 505, 315
Dame T. M. et al., 1987, 322, 706
Danner R., 1998, A&AS, 128, 331
Dickey J. M., Garwood R. W., 1989, ApJ, 341, 201
Dubinski J., Narayan R., Phillips T. G., 1995, ApJ, 448, 226
Fujita Y., Inoue S., Nakamura T., Manmoto T., Nakamura K. E., 1998, ApJ, 495, L85
Garcia M. R., McClintock J. E., Narayan R., Callanan P., Murray S. S., 2001, ApJ, 553, L47
Grindlay J. et al., 1999, astro-ph/0005496
Grindlay J. et al., 2001, Gamma-Ray Astrophysics 2001, AIP Conf. Proceedings, in press
Grindlay J., 1978, ApJ, 221, 234
Grove J. E., Johnson W. N., Kroeger R. A., McNaron-Brown K., Skibo J. G., Phlips B. F., 1998, ApJ, 500, 899
Hansen, B. M. S., Phinney, E. S., 1997, MNRAS, 291, 569
Hawley J. F., Balbus S. A., Stone J.M., 2001, ApJ, 554, L49
Heckler A. F., Kolb E. W., 1996, ApJ, 472, L85
Iben I., Jr., Tutukov A. V., Yungelson L. R., 1995, ApJS, 100, 233
Igumenshchev I. V., Abramowicz M. A., Narayan R., 2000, ApJ, 537, L27
Igumenshchev I. V., Narayan R., 2001, astro-ph/0105365
Imanishi, K., Koyama, K., Tsuboi, Y., 2001, ApJ, 557, 747
Ipser J. R., Price R. H., 1977, ApJ, 216, 578
Ipser J. R., Price R. H., 1982, ApJ, 255, 654
Ipser J. R., Price R. H., 1983, ApJ, 267, 371
Larson R. B., 1981, MNRAS, 194, 809
Lasota J. P., 2000, A&A, 360, 575
Lasota J. P., 2001, NewAR, 45, 449
Lazarian, A., Pogosyan, D., 2000, ApJ, 537, 720
Loewenstein, M., Mushotzky, R. F., Angelini, L., Arnaud, K. A., Quataert, E., 2001, ApJ, 555, L21
Madau P., Rees M. J., 2001, ApJ, 551, L27
Maloney P. R., Colgan S. W. J., Hollenbach D. J., 1997, ApJ, 482, L41
Mao S., Smith M. C., Wozniak P., Udalski A., Szymanski M., Kubiak M., Pietrzynski G., Soszynski I., Zebrun K., 2001, astro-ph/0108312
McDowell J., 1985, MNRAS, 217, 77
Mirabel I. F., Rodríguez L. F., 1999, ARA&A, 37, 409
Morrison R., McCammon D., 1983, ApJ, 270, 119
Nelemans G., Tauris T. M., van den Heuvel E. P. J., 1999, A&A, 352, L87
Ostriker J. P., McCray R., Weaver R., Yahil A., 1976, ApJ, 208, L61
Ostriker J. P., Rees M. J., Silk J., 1970, Astrophysical Letters, 6, 179
Paczyński B., 2001, astro-ph/0107443
Popov S. B., Prokhorov M. E., 1998, A&A, 331, 535
Ruffert M., 1999, A&A, 346, 861
Rutledge R. E., Bildsten L., Brown E. F., Pavlov G. G., Zavlin V. E., 2001, ApJ, 551, 921
Rutledge R. E., Bildsten L., Brown E. F., Pavlov G. G., Zavlin V. E., 2001, ApJ, in press, astro-ph/0105319
Schwarzchild, M., Härm, R. 1959, ApJ, 129, 637
Schwope A. D., Hasinger G., Schwarz R., Haberl F., Schmidt M., 1999, A&A, 341, L51
Scoville N. Z., Sanders D. B., 1987, in Hollenbach D. J., Thronson H. A., eds., Interstellar Processes, Reidel Publishing Co., Dordrecht, p. 21
Shapiro S. L., Lightman A. P., 1976, ApJ, 204, 555
Shapiro S. L., Teukolsky S. A., 1983, Black Holes, White Dwarfs, & Neutron Stars. Wiley-Interscience, New York, NY
Shvartsman, V. F., 1971, Soviet Astronomy AJ, 14, 662
Stocke, J. T., Wang, Q. D., Perlman, E. S., Donahue, M. E., Schachter, J. F., 1995, AJ, 109, 1199
Sunyaev R., Revnivtsev M., 2000, A&A, 358, 617
Thorsett, S. E, Chakrabarty, D., 1999, ApJ, 512, 288
Treves, A., Colpi, 1991, A&A, 241, 107
Treves, A., Turolla, R., Zane, S., Colpi, M., 2000, PASP, 112, 297
van Paradijs J., 1996, ApJ, 464, L139
van Paradijs J., White, N. E., 1995, ApJ, 447, L33
Voges W. et al., 1999, A& A, 349, 389
Walter F. M., Wolk S. J., Neuhauser R., 1996, Nature, 379, 233
Wang J. C. L., 1997, ApJ, 486, L119
Watson, M. G. et al., 2001, A&A, 365, L51
White N. E., van Paradijs J., 1996, ApJ, 473, L25
Wilkes B. J. et al., 2000, astro-ph/0011377

This paper has been produced using the Royal Astronomical Society/Blackwell Science LaTeX style file.